ELSEVIER

Journal of Alloys and Compounds 450 (2008) 157–161

Journal of ALLOYS AND COMPOUNDS

www.elsevier.com/locate/jallcom

Physicochemical properties of the $EuBr_2$–KBr binary system

L. Rycerz[a], E. Ingier-Stocka[a], M. Cieslak-Golonka[a], A. Wojciechowska[a],
S. Gadzuric[b,c], M. Gaune-Escard[c,*]

[a] *Faculty of Chemistry, Wroclaw University of Technology, Wybrzeze Wyspianskiego 27, 50-370 Wroclaw, Poland*
[b] *Faculty of Natural Science, Department of Chemistry, University of Novi Sad, Trg. D. Obradovica 3, 21000 Novi Sad, Serbia*
[c] *Ecole Polytechnique, IUSTI CNRS UMR 6595, Technopole de Chateau-Gombert,*
5 rue Enrico Fermi, 13453 Marseille Cedex 13, France

Received 13 October 2006; received in revised form 31 October 2006; accepted 1 November 2006
Available online 5 December 2006

Abstract

The phase diagram of the $EuBr_2$–KBr binary system was derived from DSC measurements. It exhibits three eutectics and three stoichiometric compounds. The first compound, K_2EuBr_4, melts congruently at 834 K. The second one, $KEuBr_3$ undergoes a solid–solid phase transition at 810 K and decomposes peritectically at 846 K. The third compound, KEu_2Br_5, melts congruently at 880 K. The composition of the three eutectic mixtures, $x(EuBr_2) = 0.318$, 0.433 and 0.789, respectively, were determined by the Tamman method. The respective eutectic temperatures are 829, 811 and 854 K.

Diffuse reflectance spectra of the pure components and their solid mixtures confirmed the existence of new phases exhibiting their own spectral characteristics, which may be related to the existence of above mentioned compounds in the system under investigation.

Keywords: Phase diagram; Thermodynamic properties; Rare earth alloys and compounds; Enthalpy; Optical spectroscopy

1. Introduction

A substantial amount of thermochemical data has been reported for lanthanide dichlorides, but as with the trihalides, only estimated values were available for lanthanide dibromides [1–3]. Thermodynamic data on europium(II) bromide, i.e. temperature and enthalpy of fusion [1,2], entropy at 298 K and enthalpy of formation of solid $EuBr_2$ at 298 K [4,5] as well as heat capacity of solid and liquid europium(II) bromide [5] were reported but are estimated data only. Therefore, in view of the importance of $EuBr_2$ in many applications like, e.g. the perspective storage X-ray phosphors for visualization of the X-ray images or luminophore plate production [6–8], we have initiated a research program focussing both on $EuBr_2$ [9] and the mixtures it forms with alkali bromides. For each system, different thermodynamic properties were determined as also the corresponding equilibrium phase diagram and electrical conductivity [10–13]. The present work is devoted to phase equilibria in the $EuBr_2$–KBr system.

2. Experimental

2.1. Chemicals

Europium(II) bromide was synthesised from the oxide Eu_2O_3 (Aldrich 99.9%) by a modified Haschke and Eick method [14]. The main steps of the synthesis included: dissolution of Eu_2O_3 in hot concentrated HBr acid, crystallisation of $EuBr_3{\cdot}6H_2O$, dehydration of hexahydrate and thermal decomposition of $EuBr_3$ under reduced pressure. Chemical analysis of $EuBr_2$ obtained in this way was performed by mercurimetric (bromine) and complexometric methods (europium). Europium and bromine content (Eu 48.74%; 48.75% theoretical; Br 51.26%; 51.25% theoretical) indicate the correctness of the synthesis method.

Potassium bromide was Merck Suprapur reagent (min. 99.9%). Before use, it was progressively heated up to fusion under gaseous HBr atmosphere. Excess of HBr was then removed from the melt by argon bubbling.

Mixtures of $EuBr_2$ and KBr (in appropriate proportions) were melted in vacuum-sealed quartz ampoules, homogenised and solidified. Experimental samples were ground in an agate mortar in a glove box. Homogenous mixtures of different composition were prepared in this way and used in phase diagram and electrical conductivity measurements.

All chemicals were handled in a high purity argon atmosphere glove box (water content <1 ppm).

---

[*] Corresponding author. Tel.: +33 491 106882; fax: +33 491 117439.
E-mail address: Marcelle.Gaune-Escard@polytech.univ-mrs.fr (M. Gaune-Escard).

0925-8388/$ – see front matter © 2006 Elsevier B.V. All rights reserved.
doi:10.1016/j.jallcom.2006.11.006

2.2. Measurements

The temperatures and enthalpies of phase transitions of $EuBr_2$–KBr binary mixtures were measured with a Setaram DSC 121 differential scanning calorimeter. The apparatus and the measurement procedure were described in detail previously [15,16]. Samples of 300–500 mg were contained in quartz ampoules (about 6 mm diameter, 15 mm length) sealed under reduced pressure of argon. The sidewalls of ampoules were grounded in order to fit the cells snugly into the heat flow detector. Experiments were conducted at heating and cooling rates ranging between 5 and 0.2 K min^{-1}.

Electronic reflectance spectra of powdered samples were measured with a Carry 500 Scan UV–vis–NIR Spectrophotometer (Varian) in the 10,000–50,000 cm^{-1} range. The spectra were measured with a resolution of 10 cm^{-1}. The scan rate was 4511 cm^{-1} min^{-1}, slit width 2 nm.

The diffuse reflectance spectra were recorded for the components $EuBr_2$ and KBr, as well as for mixtures of eight compositions with $x(EuBr_2) = 0.200$, 0.333 (K_2EuBr_4), 0.400, 0.500 ($KEuBr_3$), 0.542, 0.615, 0.667 (KEu_2Br_5) and 0.773. Experimental samples were melted, homogenised, cooled and powdered prior to measurements.

3. Results and discussion

3.1. Phase diagram

DSC investigations were performed on samples with 45 compositions. The corresponding thermograms yielded both the temperature and the enthalpy change of each thermal event occuring upon heating or cooling. Enthalpy values obtained from heating and cooling runs were almost the same, the difference not exceeding 2%. However, as supercooling was observed on nearly all cooling curves, the temperature and enthalpy data reported here were taken from heating cycles only. A detailed phase diagram was obtained for the $EuBr_2$–KBr system (Fig. 1) from a thorough analysis and cross-correlation of all thermal events occuring in experimental samples.

Some characteristic DSC heating thermograms (heating rate 5 K min^{-1}) are presented in Fig. 2 and they correspond to the samples of compositions $x = 0.146$, 0.373, 0.622 and 0.804 (x denotes $EuBr_2$ mole fraction). In all these heating runs, the effect at the highest temperature corresponded to the liquidus temperature of each sample.

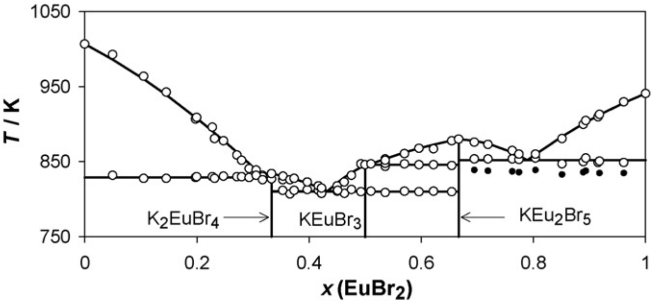

Fig. 1. Phase diagram of $EuBr_2$–KBr binary system.

In the composition range $0 < x < 0.333$, two endothermic peaks were present in all heating thermograms (for example Fig. 2a, $x = 0.145$). The first one, at 829 K, could be undoubtedly ascribed to the KBr–K_2EuBr_4 eutectic effect. As quoted previously, the second effect corresponded to the liquidus temperature. The eutectic contribution to the enthalpy of fusion was determined and plotted against composition in Fig. 3a. This so-called Tamman construction made it possible to evaluate the eutectic composition accurately from the intercept of the two linear parts in Fig. 3a, as $x = 0.318$. The KBr–K_2EuBr_4 eutectic mixture melts with the enthalpy $\Delta_{fus}H_m \approx 16.8$ kJ mol^{-1}. In this Tamman construction it was assumed that there was no solubility in the solid state. Thus the straight lines intercepted the composition axis at $x = 0.0$ and 0.333.

For the mixture of composition $x = 0.333$ only a single effect at 834 K was observed on thermograms, which had a characteristic shape, typical of a congruently melting compound. From the above observations, we deduced the existence of the K_2EuBr_4 congruently melting compound in the $EuBr_2$–KBr system.

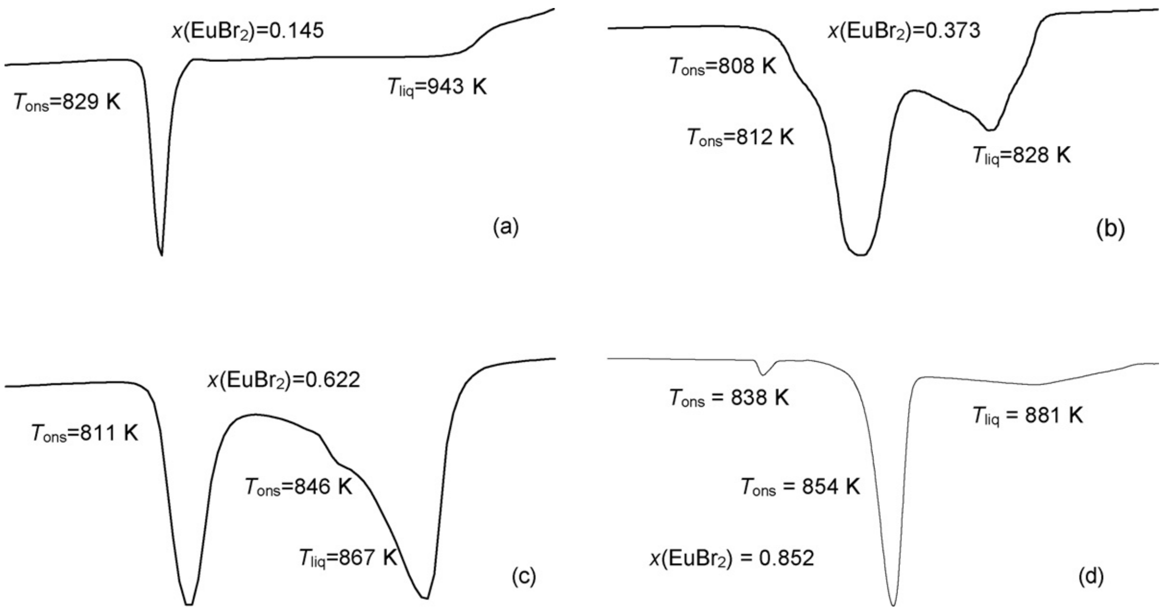

Fig. 2. DSC heating curves for selected $xEuBr_2–(1-x)KBr$ mixtures ($x = 0.145$, 0.373, 0.622 and 0.852); heating rate = 5 K min^{-1}.

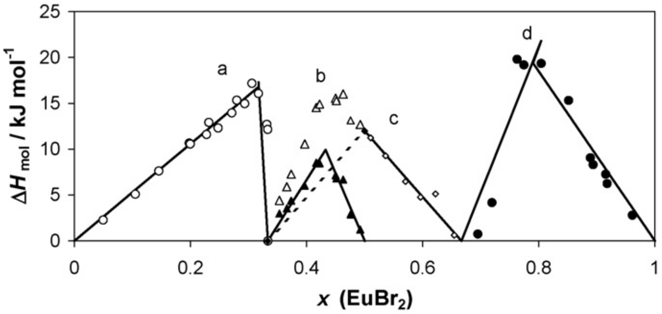

Fig. 3. Determination of eutectics in $EuBr_2$–KBr binary system by Tamman diagrams (detailed description in the text). (a) KBr–K_2EuBr_4 eutectic—open circles: enthalpy of effects related to the eutectic ($x_{eut} = 0.318$, $T_{eut} = 829$ K); (b) graphical evaluation of the K_2EuBr_4–$KEuBr_3$ eutectic—open triangles: global enthalpy related to eutectic and $KEuBr_3$ transition or formation; black triangles: calculated enthalpy related to K_2EuBr_4–$KEuBr_3$ eutectic ($x = 0.433$, $T_{eut} = 811$ K); (c) $KEuBr_3$ transition or formation—open diamonds: enthalpy related to the compound formation or transition in composition range $0.500 \leq x < 0.666$; broken line: calculated enthalpy related to the compound transition in composition range $0.333 < x \leq 0.500$; (d) KEu_2Br_5–$EuBr_2$ eutectic—black circles: enthalpy of effects related to the eutectic ($x_{eut} = 0.789$, $T_{eut} = 852$ K); solid lines: linear regression of experimental results.

Three endothermic effects were present in all heating thermograms in the composition range $0.333 < x < 0.666$ (Fig. 2b and c, $x = 0.373$ and 0.622). Here also the highest temperature corresponded to the liquidus. The thermal event at 846 K took place in all samples with $0.500 < x < 0.666$ (Fig. 2c, $x = 0.622$). Its characteristic shape (overlapping with liquidus effect) suggests that it can be ascribed to $KEuBr_3$ peritectical decomposition.

In the very narrow temperature range 808–812 K, several phase equilibria take place over the composition range $0.333 < x < 0.666$. However, their number may be difficult to appreciate sometimes. For this reason, we performed more detailed investigations on this composition range by running DSC scans at far smaller heating rates (1 and 0.2 K min^{-1}). For samples of composition $0.500 \leq x < 0.666$ only a single thermal effect was found at 810 K (Fig. 4b), whereas in the range $0.333 < x < 0.500$ the effect also observed around 810 K resulted actually from the superposition of two effects, i.e. at 810 and 811 K, respectively as shown in Fig. 4a. Unfortunately, these two merged thermal events could not be fully resolved even upon very slow heating (0.2 K min^{-1}). However even so, two characteristic temperatures (810 and 811 K) were determined in all samples in the composition range $0.333 < x < 0.500$ and only one (810 K) at compositions beyond. Effect at 810 K was assigned to the solid-solid transition of the $KEuBr_3$ compound. Accordingly, the thermal event at 811 K should be related to the K_2EuBr_4–$KEuBr_3$ eutectic.

The evaluation of this eutectic mixture composition from an enthalpy versus composition plot, as explained above, would not be reliable in view of the merged and non-separable enthalpy effects observed in the narrow temperature range 810–811 K. An alternate method was used instead. The global enthalpy related to the overlapping effects, ΔH_m (global), was determined from DSC thermograms obtained at heating rate 5 K min^{-1}. The enthalpy related to the eutectic, ΔH_m (eutectic) can be calculated as:

$$\Delta H_m(\text{eutectic}) = \Delta H_m(\text{global}) - \Delta H_m(\text{KEuBr}_3\ \text{trs}) \tag{1}$$

The contribution of the enthalpy of transition, ΔH_m ($KEuBr_3$ trs), to the global enthalpy could be determined from a Tamman diagram (Fig. 3c). The effect at 810 K observed in the range $0.500 \leq x < 0.666$ results only from the solid–solid phase transition in $KEuBr_3$. So the related enthalpy varies linearly with composition:

$$\Delta H_m(\text{KEuBr}_3\ \text{trs}) = 47.97 - 71.96x \tag{2}$$

with the maximal value 11.99 kJ mol^{-1} at $x = 0.500$. The linear dependence must occur also for $x < 0.500$. As the thermal effect related to this transition disappears at $x = 0.333$, thus at $x = 0.333$ this enthalpy value must be equal 0 kJ mol^{-1}. Using the enthalpy values at $x = 0.500$ (11.99 kJ mol^{-1}) and $x = 0.333$ (0 kJ mol^{-1}) (black diamonds in Fig. 3c) ΔH_m ($KEuBr_3$ trs) was fitted to the linear equation ($0.333 \leq x \leq 0.500$):

$$\Delta H_m(\text{KEuBr}_3\ \text{trs}) = 71.79x - 23.91 \tag{3}$$

and plotted against x in Fig. 3c (dashed line).

By introducing Eqs. (3) into (1), it was possible to calculate the enthalpy change related to the K_2EuBr_4–$KEuBr_3$ eutectic (Fig. 3b, black triangles). The eutectic composition ($x = 0.433$) was determined from the intercept of the two linear parts in Fig. 3b, the related fusion enthalpy $\Delta_{fus}H_m$ is about 9.9 kJ mol^{-1}.

For the mixture of composition $x = 0.666$ only one effect was observed on thermograms at 880 K with a characteristic shape, typical of a congruently melting compound. From the above observations, we deduced the existence of the KEu_2Br_5 congruently melting compound in the $EuBr_2$–KBr system.

Three endothermic peaks were present in all heating thermograms in the composition range $0.666 < x < 1.0$ (Fig. 2d, $x = 0.852$). The effect at the highest temperature corresponds to the liquidus. Effect at 854 K could be undoubtedly ascribed

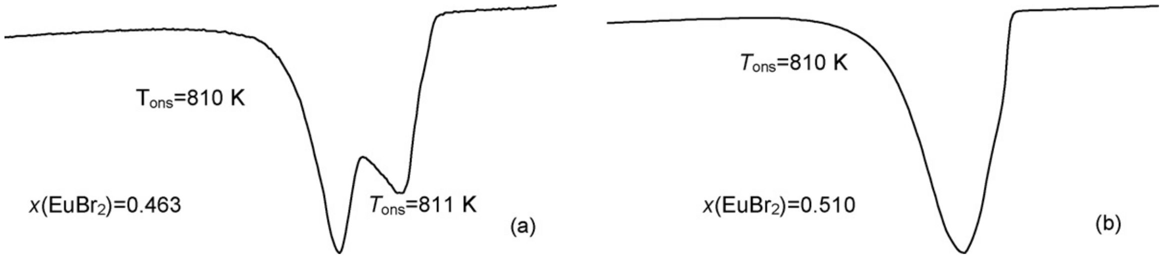

Fig. 4. DSC heating curves for selected xEuBr$_2$–$(1-x)$KBr mixtures ($x = 0.463$ and 0.510): heating rate = 0.1 K min^{-1}.

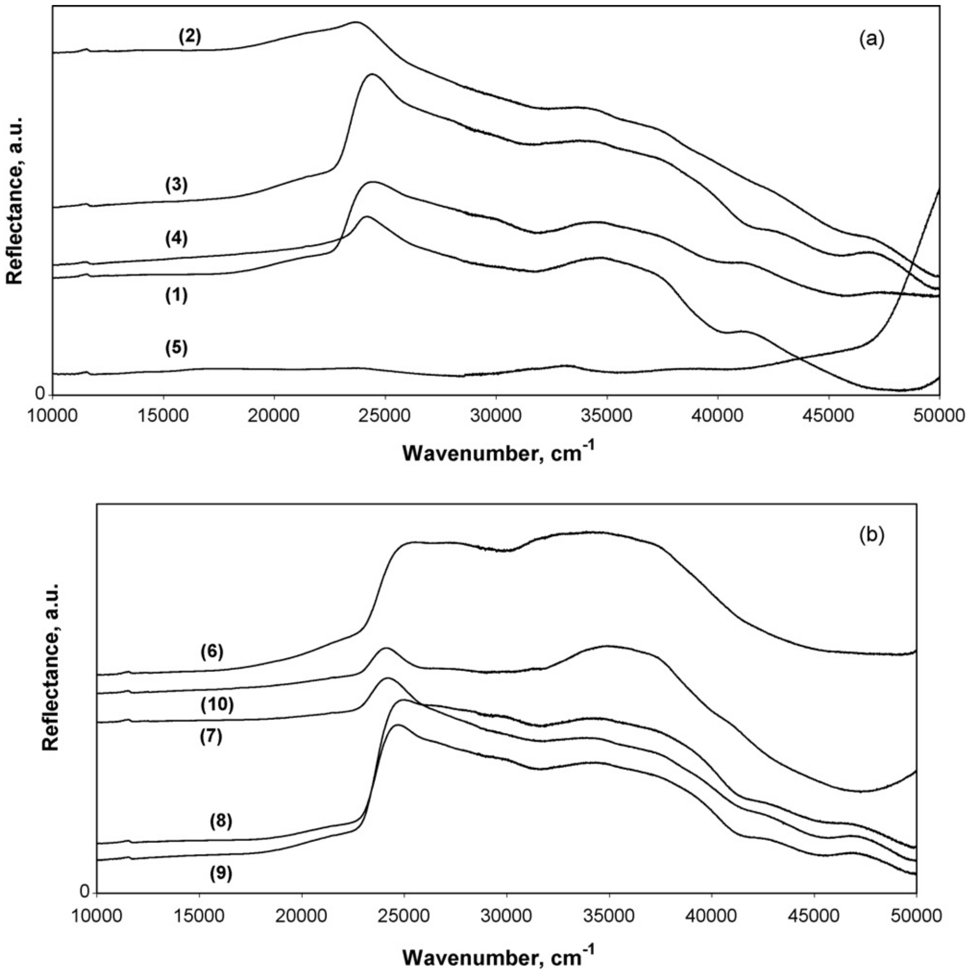

Fig. 5. Reflectance spectra of powdered samples: (a) KEu_2Br_5 **(1)**, K_2EuBr_4 **(2)**, $KEuBr_3$ **(3)**, pure $EuBr_2$ **(4)** and pure KBr **(5)**; (b) $x = 0.200$ **(6)**, $x = 0.400$ **(7)**, $x = 0.542$ **(8)**, $x = 0.615$ **(9)** and $x = 0.773$ **(10)**.

to the KEu_2Br_5–$EuBr_2$ eutectic. Eutectic contribution to the enthalpy of fusion was determined and plotted against composition in Fig. 3d. Eutectic composition was evaluated accurately, from the intercept of the two linear parts in Fig. 3d as $x = 0.789$. The KEu_2Br_5–$EuBr_2$ eutectic mixture melts with the enthalpy $\Delta_{fus}H_m \approx 19.4\,kJ\,mol^{-1}$. The straight lines intercepted the composition axis at $x = 0.666$ and 1.

The origin of the additional and weak thermal effect (less than $0.7\,kJ\,mol^{-1}$), observed in DSC thermograms at 838 K (Fig. 2d) for all mixtures in the composition range $0.7 < x < 1$ (black points in Fig. 1) cannot be explained at the present time. Additional information is expected from structural studies, which are planned in the nearest future.

3.2. Electronic spectra of $EuBr_2$–KBr solid mixtures

In order to confirm the reliability of the constructed phase diagram, the electronic spectra were measured for several $EuBr_2$ and KBr mixtures. According to the phase diagram determined from DSC measurements, the existence of three compounds, i.e. KEu_2Br_5 **(1)**, K_2EuBr_4 **(2)** and $KEuBr_3$ **(3)** was assumed. Due to the lack of information concerning spectroscopic properties of $EuBr_2$–KBr mixtures, the reflectance spectra of the above compounds as well as pure $EuBr_2$ **(4)** and KBr **(5)** were recorded. These spectra (Fig. 5a) were used as "reference" for the spectra of the $EuBr_2$–KBr mixtures with other composition.

The first coordination sphere of the respective europium(II) containing species taken as reference can be defined as $[EuBr_2Br']$, $[EuBr_4]$ and $[EuBr_3]$ in binuclear **(1)**, monomer **(2)** and monomer **(3)**, respectively. That means that similar spectral pattern for **(1)** and **(3)**, with slight changes for **(1)** owing the presence of the Eu–Br′–Eu bridge in binuclear form, should be expected. In contrast, the spectra of compound **(2)** containing the $EuBr_4$ chromophore should differ from those spectra obtained for **(1)** and **(3)**. The analysis of the spectra shown in Fig. 5a confirmed these expectations, as detailed below.

The ultraviolet region of the $EuBr_2$ spectrum contains two distinct, broad optical absorption bands at $24{,}000$–$32{,}000\,cm^{-1}$ (I) and $34{,}000$–$44{,}000\,cm^{-1}$ (II), respectively [16]. In diffuse reflectance technique applied in this work, absorption bands for $EuBr_2$ **(4)** were observed at $23{,}000$–$33{,}000\,cm^{-1}$ and $33{,}000$–$45{,}000\,cm^{-1}$ with maximum at ca. 24,000 and $34{,}500\,cm^{-1}$ for band (I) and (II), respectively. The origin of the band are the Laporte rule allowed $4f^7 \rightarrow 4f^65d^1$ transitions in the Eu(II) ion [6,11,16–19]. Moreover, in high energetic region of the spectrum, the Br → Eu charge transfer (CT) transition can be expected. The band at ca. 41,750 cm^{-1} can be assigned to the charge transfer $Br \rightarrow Eu^{2+}$ transition. Indeed, applying the known Jørgensen formula: $\nu_{CT} = 300,000\ [\chi_{opt}(Br^-) - \chi_{opt}(Eu^{2+})]$, the $\chi_{Eu} = 1.2$ in accordance with the literature [20]. Thus, this band can be assigned to Br → Eu CT transition.

The comparison of the $EuBr_2$ spectra **(4)** with those relative to KEu_2Br_5 **(1)**, K_2EuBr_4 **(2)** and $KEuBr_3$ **(3)** shows the same general pattern with some changes characteristic of the particular compound. As bands (I) and (II) were assigned to crystal field (CF) splitting and the difference in band positions in the assumed cubic field [16] is equal to $\Delta = t_{2g} - e_g$, the magnitude of crystal field strength in the particular chromophore can be calculated.

The maximum of most prominent band (I) at ca. 25,000 cm^{-1}, which corresponds to the transition to t_{2g} level, was found to be changed as follows:

KEu_2Br_5 **(1)**: 24,580 $cm^{-1} \cong KEuBr_3$ **(3)**: 24,500 $cm^{-1} \gg K_2EuBr_4$ **(2)**: 23,865 cm^{-1}, just as expected (vide infra). Moreover, in $EuBr_2$ **(4)** spectrum the maximum of the first band being 24,260 cm^{-1} indicates different CF strength. In accordance with literature data [16], the maximum of higher energy band (II) (transition to the e_g level) is practically the same for all above compounds. It is situated at about 34,400–34,600 cm^{-1}. The 10 Dq (Δ) values (in cm^{-1}) were obtained as 10,080, 10,560, 9900 and 10,400 for **(1)**, **(2)**, **(3)** and **(4)** compounds, respectively. That means that the splitting parameter Δ for KEu_2Br_5 **(1)** and $KEuBr_3$ **(3)** was found to be slightly smaller than for $EuBr_2$ **(4)** (9900, 10,080 and 10,400 cm^{-1}, respectively), whereas K_2EuBr_4 **(2)** creates crystal field stronger (10,560 cm^{-1}) than $EuBr_2$. Thus, the crystal field parameters different for each compound can be also an indication for various species present in the system.

Generally, the Δ values found in this work are several hundred cm^{-1} lower than the corresponding value found for $EuBr_2$ doped KBr single crystals (11,300 cm^{-1}) [16]. This can be related to the technique, i.e. diffuse reflectance used in this work instead of absorption spectra of single crystal [16].

Fig. 5b shows the spectra of the remaining samples with various amount of $EuBr_2$, i.e. $x(EuBr_2) = 0.200$ **(6)**, 0.400 **(7)**, 0.542 **(8)**, 0.615 **(9)** and 0.773 **(10)**. On the basis of the determined phase diagram (Fig. 1) it can be expected that the spectra of the respective samples will be similar: **(6)** to K_2EuBr_4 **(2)**, **(7)** to K_2EuBr_4 **(2)** and/or $KEuBr_3$ **(3)**, **(8)** and **(9)** to KEu_2Br_5 **(1)** and/or $KEuBr_3$ **(3)** as well as **(10)** to KEu_2Br_5 **(1)** and/or $EuBr_2$ **(4)**.

As band (I) was found to be sensitive to the changing of the europium(II) environment (vide supra) (Fig. 5a and [17]), this transition was chosen as indicative reference in the analysis of experimental spectra. Besides, for this analysis, the general shape of each spectrum was also taken into account. In the solid mixture **(6)**, the shape of the spectrum was found to be similar to $EuBr_2$ in KBr matrix [16]. However, band (I) was strongly shifted hypsochromically up to 25,510 cm^{-1}in contrast to all other investigated samples, which may suggest the presence of unknown species. Moreover, the Δ value was found to be 8640 cm^{-1}. This value appears to be the smallest among all studied species. For mixture **(7)** both the shape and the band positions resemble those found for $KEuBr_3$, thus suggesting the presence of such compound in the mixture. The spectra of **(8)** and **(9)** are very similar to the spectrum of KEu_2Br_5 **(1)**. Finally, the spectrum of **(10)** containing 77.3 mol% of $EuBr_2$ shows that this compound is a dominating one.

Summing up, the comparative studies of the electronic spectra of $EuBr_2$–KBr mixtures of different compositions supported the existence of $KEuBr_3$ and KEu_2Br_5 in the $EuBr_2$–KBr phase diagram. In the KBr-rich range, the only composition investigated **(6)** did not lead to definitive conclusion in view of the spectrum complexity, indeed this spectrum was rather different from that obtained for the K_2EuBr_4 adjacent compound, thus suggesting the posible existence of other species. Therefore other more suitable techniques would have to be used to get a more detailed picture of the $EuBr_2$–KBr mixtures in KBr-rich region.

References

[1] C.E. Wicks, F.E. Block, Thermodynamic Properties of 65 Elements—Their Oxides, Halides, Carbides and Nitrides, U.S. Bureau of Mines Bulletin 605, U.S. Government Printing Office, Washington, 1963.

[2] R.E. Thoma, in: L. Eyring (Ed.), Progress in the Science and Technology of the Rare Earths, vol. 2, Pergamon Press, New York, 1966, pp. 90–121.

[3] Gmelin, Handbook of Inorganic Chemistry, vol. C6, 1978, pp. 65–76.

[4] J.M. Haschke, H.A. Eick, J. Phys. Chem. 74 (1970) 1806–1808.

[5] J.M. Haschke, High Temp. Sci. 9 (1977) 77–84.

[6] Yu.V. Zorenko, R.M. Turchlak, W. Gryk, M. Grinberg, J. Lumin. 106 (2004) 313–320.

[7] U.S. Application 20040126489.

[8] U.S. Patent 7,038,221.

[9] L. Rycerz, S. Gadzuric, E. Ingier-Stocka, R.W. Berg, M. Gaune-Escard, J. Nucl. Mater. 344 (2005) 115–119.

[10] S. Gadzuric, E. Ingier-Stocka, L. Rycerz, M. Gaune-Escard, J. Alloys Compd. 397 (2005) 63–67.

[11] E. Ingier-Stocka, S. Gadzuric, L. Rycerz, M. Cieslak-Golonka, M. Gaune-Escard, J. Nucl. Mater. 344 (2005) 120–123.

[12] L. Rycerz, S. Gadzuric, E. Ingier-Stocka, M. Gaune-Escard, in preparation.

[13] L. Rycerz, S. Gadzuric, E. Ingier-Stocka, M. Gaune-Escard, in preparation.

[14] J.M. Haschke, H.A. Eick, J. Inorg. Nucl. Chem. 32 (1970) 2153–2158.

[15] M. Gaune-Escard, L. Rycerz, W. Szczepaniak, A. Bogacz, J. Alloys Compd. 204 (1994) 193–196.

[16] A. Hernandez, W.K. Cory, J. Rubio, J. Chem. Phys. 72 (1) (1980) 198–205.

[17] C. Wickleder, J. Alloys Compd. 300–301 (2000) 193–198; C. Wickleder, J. Alloys Compd. 374 (2004) 10–13.

[18] C. Wickleder, Z. Naturforsch 57B (2002) 901–907.

[19] C. Wickleder, Z. Anorg. Allgem. Chem. 628 (2002) 1815–1820.

[20] A.B.P. Lever, Inorganic Electronic Spectroscopy, 2nd ed., Elsevier, Amsterdam, 1984.